Structural Engineering and Mechanics, *Vol. 55, No. 1 (2015) 29-46*
DOI: http://dx.doi.org/10.12989/sem.2015.55.1.029

Vibrations of truncated shallow and deep conical shells with non-uniform thickness

Jae-Hoon Kang*

Department of Architectural Engineering, Chung-Ang University,
221 Heuksuk-Dong, Dongjak-Ku, Seoul, 156-756, Republic of Korea

(Received July 13, 2014, Revised November 3, 2014, Accepted November 6, 2014)

Abstract. A three-dimensional (3-D) method of analysis is presented for determining the natural frequencies of a truncated shallow and deep conical shell with linearly varying thickness along the meridional direction free at its top edge and clamped at its bottom edge. Unlike conventional shell theories, which are mathematically two-dimensional (2-D), the present method is based upon the 3-D dynamic equations of elasticity. Displacement components u_r, u_θ, and u_z in the radial, circumferential, and axial directions, respectively, are taken to be periodic in θ and in time, and algebraic polynomials in the r and z directions. Strain and kinetic energies of the truncated conical shell with variable thickness are formulated, and the Ritz method is used to solve the eigenvalue problem, thus yielding upper bound values of the frequencies by minimizing the frequencies. As the degree of the polynomials is increased, frequencies converge to the exact values. Convergence to four-digit exactitude is demonstrated. The frequencies from the present 3-D method are compared with those from other 3-D finite element method and 2-D shell theories.

Keywords: truncated conical shell; vibration; variable thickness; three-dimensional analysis

1. Introduction

Conical shells play an important role in many industrial fields and are widely used as structural components of loudspeakers, aircrafts, space vehicles, and so on. However, the vibration of truncated conical shells has been studied to a lesser extent than that of cylindrical shells because of the greater mathematical complexity involved in characterizing their geometry and dynamic behavior, and the greater difficulty in solving the governing equations.

Most of the existing literature describes the vibration analysis for *thin* conical shells with *uniform* thickness and is based on a thin shell or membrane type of two-dimensional (2-D) shell theory (Leissa 1993). Even though the analysis is based on 2-D classical thin shell theory, sufficient engineering data have not been obtained since the analysis requires considerable analytical labor and computational time.

Recently, Qu *et al*. (2013a, b) describe a variational general formulation for predicting the free, steady-state and transient vibration analyses of functionally graded conical shells of revolution

*Corresponding author, Professor, E-mail: jhkang@cau.ac.kr

http://www.techno-press.org/?journal=sem&subpage=8 ISSN: 1225-4568 (Print), 1598-6217 (Online)

subjected to various combinations of classical and non-classical boundary conditions. Jin *et al*. (2014) developed a unified modified Fourier solution based on the first order shear deformation theory for the vibrations of various composite laminated structure elements of revolution with general elastic restraints including conical shells. Sofiyev (2014a) investigated the large-amplitude vibration of non-homogenous orthotropic composite truncated conical shell, and he (2014b) also analyzed the non-linear vibration of laminated non-homogenous orthotropic truncated conical shell.

Three-dimensional (3-D) analysis of structural elements has long been a goal of those who work in the field. With the current availability of computers of increased speed and capacity, it is now possible to perform 3-D structural analyses of bodies to obtain accurate values of static displacements, free vibration frequencies and mode shapes, and buckling loads and mode shapes.

The literature that addresses the free vibration of truncated conical shells based on 3-D analyses is quite limited. The first contribution to the 3-D analysis of the truncated conical shells was by Leissa and So (1995). Buchanan (2000) and Buchanan and Wong (2001) analyzed the truncated conical shells by a 3-D finite element method. However, the above mentioned works (Leissa and So 1995, Buchanan 2000, Buchanan and Wong 2001) were all confined to *uniform* shell thickness, and were all based upon the conical coordinate system. Recently, a 3-D free vibration analysis of the functionally graded truncated conical shells subjected to thermal environment was presented using the differential quadrature method (Malekzadeh *et al*. 2012). The study on the vibrations of truncated conical shells with variable thickness having various boundary conditions based on the circular cylindrical coordinate system from a 3-D theory has not been reported.

In the present study, a 3-D analysis on the vibrations of a truncated conical shell with linear thickness variation free at the top edge and clamped at the bottom edge is presented. Instead of attempting to solve the equations of motion, an energy approach is applied. Recently, an energy-oriented modified Fourier method can also be used to solve the tiled problem. Vibration of 2-D and 3-D plates, cylindrical, conical and spherical shells with general boundary conditions has been carried out by this method (Jin *et al.* 2013a, Jin *et al.* 2013b, Ye *et al.* 2013, Jin *et al.* 2014a, Jin *et al.* 2014b, Jin *et al.* 2014c, Su *et al.* 2014a, Su *et al.* 2014b, Ye *et al.* 2014).

The analysis uses the 3-D equations of the theory of elasticity in their general forms for isotropic materials. They are only limited to small strains. No other constraints are placed on the displacements. This is an obvious difference between the 3-D analysis and the classical 2-D thin shell theories, which make very limiting assumptions about the displacement variation through the shell thickness. Therefore the present 3-D method can be applied to very thick shells as well as thin shells.

To evaluate the energy integrations over the truncated conical shell volume, displacements and strains are expressed in terms of the circular cylindrical coordinates, instead of the conical coordinate system or related 3-D shell coordinates which are normal and tangent to the shell mid-surface, mainly because it takes more time to compute the energy integration numerically based on the 3-D shell coordinates than based on the circular cylindrical coordinates. The frequencies from the present 3-D method are also compared with results from other 3-D finite element method and 2-D thin shell theories.

2. Method of analysis

A representative cross-section of a truncated conical shell with linear thickness variation along

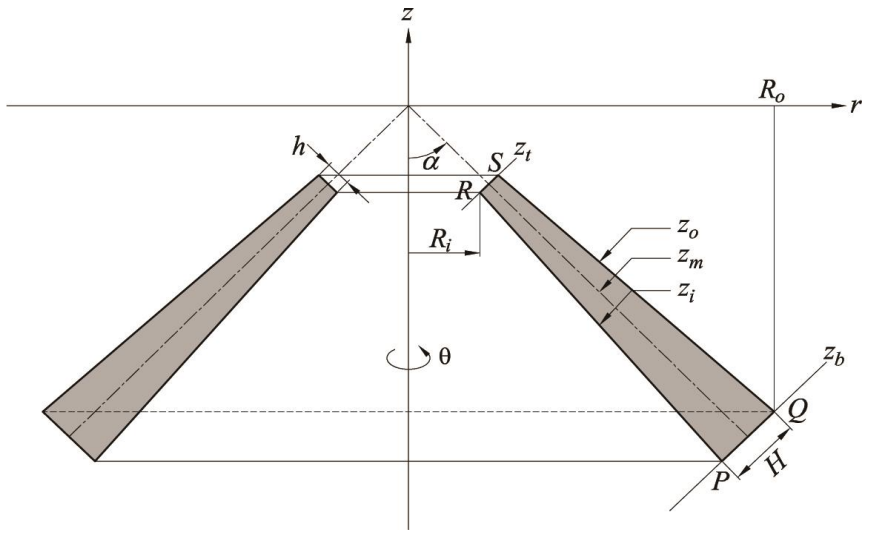

Fig. 1 A representative cross-section of a truncated conical sell of revolution with linear thickness variation along the meridional direction, and the cylindrical coordinate system (r, θ, z)

the meridional direction with the vertex half-angle α, the inner radius of the top edge R_i, and the outer radius of the bottom edge R_o is shown in Fig. 1. The thicknesses at its top and bottom edges are h and H, respectively. The circular cylindrical coordinate system (r, θ, z), also shown in the figure, is used in the analysis, where θ is the circumferential angle. The coordinates of the points P, Q, R, and S in the figure are P=(P_r, P_z), Q=(Q_r, Q_z), R=(R_r, R_z), and S=(S_r, S_z). The origin of the (r, z) coordinates is located at the vertex of the mid-surface of the conical shell. The truncated conical shell of revolution is obtained by rotating the cross-section for $r \geq 0$ in Fig. 1 360° about the z-axis. The straight lines $z_{i,m,o}$ in Fig. 1 are the inner, middle, and outer surfaces of the truncated conical shell, respectively, and their equations are expressed as

$$z_m = -r\cot\alpha\,, \tag{1}$$

$$z_i = \frac{P_z - R_z}{P_r - R_r}(r - R_r) + R_z\,, \tag{2}$$

$$z_o = \frac{Q_z - S_z}{Q_r - S_r}(r - S_r) + S_z\,, \tag{3}$$

where

$$P_r = R_o - H\cos\alpha\,, \tag{4}$$

$$P_z = \frac{3H\cos^2\alpha - 2R_o\cos\alpha - H}{2\sin\alpha}\,, \tag{5}$$

$$Q_r = R_o\,, \tag{6}$$

$$Q_z = -\frac{H\cos^2\alpha + 2R_o\cos\alpha - H}{2\sin\alpha}\,, \tag{7}$$

$$R_r = R_i\,, \tag{8}$$

$$R_z = \frac{h\cos^2\alpha - 2R_i\cos\alpha - h}{2\sin\alpha}\,, \tag{9}$$

$$S_r = R_i + h\cos\alpha\,, \tag{10}$$

$$S_z = -\frac{3h\cos^2\alpha + 2R_i\cos\alpha - h}{2\sin\alpha}\,. \tag{11}$$

The top and bottom edges $z_{t,b}$ are normal to the mid-surface of the shell and their equations are expressed as

$$z_t = (r - R_r)\tan\alpha + R_z\,, \tag{12}$$

$$z_b = (r - P_r)\tan\alpha + P_z\,. \tag{13}$$

The domain (Λ) of the truncated conical shell of revolution is described by

$$R_r \le r \le S_r\,,\quad z_i \le z \le z_t\,,\quad 0 \le \theta \le 2\pi\,, \tag{14}$$

and

$$S_r \le r \le P_r\,,\quad z_i \le z \le z_o\,,\quad 0 \le \theta \le 2\pi\,, \tag{15}$$

and

$$P_r \le r \le Q_r\,,\quad z_b \le z \le z_o\,,\quad 0 \le \theta \le 2\pi\,. \tag{16}$$

The domain (Λ) expressed in terms of the non-dimensional circular cylindrical coordinates (ψ, θ, ζ), defined by $\psi \equiv r/R_o$ and $\zeta \equiv z/H$, is given by

$$R_r^* \le \psi \le S_r^*\,,\quad \zeta_i \le \zeta \le \zeta_t\,,\quad 0 \le \theta \le 2\pi\,, \tag{17}$$

and

$$S_r^* \le \psi \le P_r^*\,,\quad \zeta_i \le \zeta \le \zeta_o\,,\quad 0 \le \theta \le 2\pi\,, \tag{18}$$

and

$$P_r^* \le \psi \le Q_r^*\,,\quad \zeta_b \le \zeta \le \zeta_o\,,\quad 0 \le \theta \le 2\pi\,, \tag{19}$$

where

$$P_r^* = P_r / R_o = 1 - H^*\cos\alpha\,, \tag{20}$$

$$Q_r^* = Q_r / R_o = 1, \tag{21}$$

$$R_r^* = R_i^* = R_i / R_o\,, \tag{22}$$

$$S_r^* = S_r / R_o = R_i^* + h^* H^*\cos\alpha\,, \tag{23}$$

and

$$\zeta_i = z_i / H = \frac{P_z^* + R_z^*}{P_r^* - R_r^*}(\psi - R_r^*) + R_z^*, \tag{24}$$

$$\zeta_o = z_o / H = \frac{Q_z^* - S_z^*}{Q_r^* - S_r^*}(\psi - S_r^*) + S_z^*, \tag{25}$$

$$\zeta_t = z_b / H = (\psi - R_r^*)\tan\alpha / H^* + R_z^*, \tag{26}$$

$$\zeta_b = z_b / H = (\psi - P_r^*)\tan\alpha / H^* + P_z^*. \tag{27}$$

with

$$H^* = H / R_o, \tag{28}$$

$$h^* = h / H, \tag{29}$$

and

$$P_z^* = P_z / H = \frac{2H^*\cos^2\alpha - 2\cos\alpha - H^*}{2H^*\sin\alpha}, \tag{30}$$

$$Q_z^* = Q_z / H = \frac{H^* - 2\cos\alpha}{2H^*\sin\alpha}, \tag{31}$$

$$R_z^* = R_z / H = -\frac{h^*H^* + 2R_i^*\cos\alpha}{2H^*\sin\alpha}, \tag{32}$$

$$S_z^* = S_z / H = \frac{h^*H^* - 2R_i^*\cos\alpha - 2h^*H^*\cos^2\alpha}{2H^*\sin\alpha}. \tag{33}$$

Employing tensor analysis, the three equations of motion in terms of the circular cylindrical coordinate system (r, θ, z) are found to be

$$\begin{aligned}
\sigma_{rr,r} + \sigma_{rz,z} + (\sigma_{rr} - \sigma_{\theta\theta} + \sigma_{r\theta,\theta})/r &= \rho\ddot{u}_r, \\
\sigma_{rz,r} + \sigma_{zz,z} + (\sigma_{rz} + \sigma_{z\theta,\theta})/r &= \rho\ddot{u}_z, \\
\sigma_{r\theta,r} + \sigma_{z\theta,z} + (2\sigma_{r\theta} + \sigma_{\theta\theta,\theta})/r &= \rho\ddot{u}_\theta,
\end{aligned} \tag{34}$$

where the σ_{ij} are the normal ($i=j$) and shear ($i\neq j$) stress components; u_r, u_z, and u_θ are the displacement components in the r, z, and θ directions, respectively; ρ is mass density per unit volume; the commas (,) indicate spatial derivatives; and the dots (.) denote time derivatives. The well-known relationships between the tensorial stresses (σ_{ij}) and strains (ε_{ij}) of isotropic, linear elasticity are

$$\sigma_{ij} = \lambda\varepsilon\delta_{ij} + 2G\varepsilon_{ij}, \tag{35}$$

where λ and G are the Lamé parameters, expressed in terms of Young's modulus (E) and Poisson's ratio (ν) for an isotropic solid as

$$\lambda = E\nu/(1+\nu)(1-2\nu), \quad G = E/2(1+\nu), \tag{36}$$

$\varepsilon \equiv \varepsilon_{rr} + \varepsilon_{zz} + \varepsilon_{\theta\theta}$ is the trace of the strain tensor, and δ_{ij} is Kronecker's delta. The 3-D tensorial strains

(ε_{ij}) are related to the three displacements u_r, u_z, and u_θ, by

$$\varepsilon_{rr} = u_{r,r}, \quad \varepsilon_{zz} = u_{z,z}, \quad \varepsilon_{\theta\theta} = (u_r + u_{\theta,\theta})/r,$$

$$2\varepsilon_{rz} = u_{r,z} + u_{z,r}, \quad 2\varepsilon_{r\theta} = u_{\theta,r} + (u_{r,\theta} - u_\theta)/r, \quad 2\varepsilon_{z\theta} = u_{\theta,z} + u_{z,\theta}/r. \tag{37}$$

Substituting Eqs. (35) and (37) into Eqs. (34), one obtains a set of three second-order partial differential equations in u_r, u_z, and u_θ governing the free vibrations. However, in the case of the conical shell, exact solutions are intractable because of the variable coefficients that appear in many terms. Alternatively, one may approach the problem from an energy perspective.

During vibratory deformation of the body, its strain energy (V) is the integral over the domain (Λ)

$$V = \frac{1}{2}\iiint_{\Lambda} [\sigma_{rr}\varepsilon_{rr} + \sigma_{zz}\varepsilon_{zz} + \sigma_{\theta\theta}\varepsilon_{\theta\theta} + 2(\sigma_{rz}\varepsilon_{rz} + \sigma_{r\theta}\varepsilon_{r\theta} + \sigma_{z\theta}\varepsilon_{z\theta})]\, r\,dr\,dz\,d\theta. \tag{38}$$

Substituting Eq. (35) into Eq. (38) results in the strain energy (V) in terms of the strains

$$V = \frac{1}{2}\iiint_{\Lambda} [\lambda(\varepsilon_{rr} + \varepsilon_{zz} + \varepsilon_{\theta\theta})^2 + 2G\{\varepsilon_{rr}^2 + \varepsilon_{zz}^2 + \varepsilon_{\theta\theta}^2 + 2(\varepsilon_{rz}^2 + \varepsilon_{z\theta}^2 + \varepsilon_{r\theta}^2)\}]\, r\,dr\,dz\,d\theta \tag{39}$$

where the tensorial strains ε_{ij} are expressed in terms of the three displacements by Eqs. (37).

The kinetic energy (T) is simply

$$T = \frac{1}{2}\iiint_{\Lambda} \rho(\dot{u}_r^2 + \dot{u}_z^2 + \dot{u}_\theta^2)\, r\,dr\,dz\,d\theta. \tag{40}$$

For the free, undamped vibration, the time (t) response of the three displacements is sinusoidal and, moreover, the circular symmetry of the body of revolution allows the displacements to be expressed by

$$\begin{aligned} u_r(\psi,\theta,\zeta,t) &= U_r(\psi,\zeta)\cos n\theta \sin(\omega t + \beta), \\ u_z(\psi,\theta,\zeta,t) &= U_z(\psi,\zeta)\cos n\theta \sin(\omega t + \beta), \\ u_\theta(\psi,\theta,\zeta,t) &= U_\theta(\psi,\zeta)\sin n\theta \sin(\omega t + \beta), \end{aligned} \tag{41}$$

where U_r, U_z, and U_θ are displacement functions of ψ and ζ, ω is a natural frequency, and β is an arbitrary phase angle determined by the initial conditions. The circumferential wave number is taken to be an integer (n=0, 1, 2, …, ∞), to ensure periodicity in θ. It may be verified by substituting the displacements into the 3-D equations of motion that the variables separable form of Eqs. (41) does apply. Then Eqs. (41) account for all free vibration modes except for the torsional ones. These modes arise from an alternative set of solutions which are the same as Eqs. (41), except that cos$n\theta$ and sin$n\theta$ are interchanged. For $n\geq 1$, this set duplicates the solutions of Eqs. (41), with the symmetry axes of the mode shapes being rotated. But for n=0 the alternative set reduces to u_r=u_z=0, $u_\theta = U_\theta^*(\psi,\varsigma)\sin(\omega t + \beta)$, which corresponds to the torsional modes. The displacements uncouple by circumferential wave number (n), leaving only coupling in r (or ψ) and z (or ζ).

The Ritz method uses the maximum potential energy ($V_{\max}$) and the maximum kinetic energy

($T_{\max}$) functionals in a cycle of vibratory motion. The functionals for the truncated conical shell with linearly varying thickness along the meridional direction in terms of the non-dimensional coordinates $\psi(\equiv r/R_o)$ and $\zeta(\equiv z/H)$ were given by

$$V_{\max} = \frac{GH}{2}\left[\int_{R_i^*}^{S_r^*}\int_{\zeta_i}^{\zeta_t} I_V\ \psi\, d\zeta\, d\psi + \int_{S_r^*}^{P_r^*}\int_{\zeta_i}^{\zeta_o} I_V\ \psi\, d\zeta\, d\psi + \int_{P_r^*}^{1}\int_{\zeta_b}^{\zeta_o} I_V\ \psi\, d\zeta\, d\psi\right], \tag{42}$$

$$T_{\max} = \frac{\rho\omega^2 H R_o^2}{2}\left[\int_{R_i^*}^{S_r^*}\int_{\zeta_i}^{\zeta_t} I_T\ \psi\, d\zeta\, d\psi + \int_{S_r^*}^{P_r^*}\int_{\zeta_i}^{\zeta_o} I_T\ \psi\, d\zeta\, d\psi + \int_{P_r^*}^{1}\int_{\zeta_b}^{\zeta_o} I_T\ \psi\, d\zeta\, d\psi\right], \tag{43}$$

where

$$I_V \equiv [(\lambda/G)(\kappa_1+\kappa_2+\kappa_3)^2 + 2(\kappa_1^2+\kappa_2^2+\kappa_3^2)+\kappa_4^2]\Gamma_1 + (\kappa_5^2+\kappa_6^2)\Gamma_2, \tag{44}$$

$$I_T \equiv (U_r^2+U_z^2)\Gamma_1 + U_\theta^2\Gamma_2, \tag{45}$$

with

$$\kappa_1 \equiv \frac{U_r + nU_\theta}{\psi},\quad \kappa_2 \equiv \frac{R_o}{H}U_{z,\zeta},\quad \kappa_3 \equiv U_{z,\zeta},$$
$$\kappa_4 \equiv \frac{R_o}{H}U_{r,\zeta} + U_{z,\psi},\quad \kappa_5 \equiv \frac{U_\theta + nU_r}{\psi} - U_{\theta,\psi},\quad \kappa_6 \equiv \frac{nU_z}{\psi} - \frac{R_o}{H}U_{\theta,\zeta}, \tag{46}$$

and Γ_1 and Γ_2 are constants, defined by

$$\Gamma_1 \equiv \int_0^{2\pi}\cos^2 n\theta = \begin{cases} 2\pi & \text{if } n=0 \\ \pi & \text{if } n\geq 1 \end{cases}, \qquad \Gamma_2 \equiv \int_0^{2\pi}\sin^2 n\theta = \begin{cases} 0 & \text{if } n=0 \\ \pi & \text{if } n\geq 1 \end{cases}. \tag{47}$$

From Eqs. (36) it is seen that the non-dimensional constant λ/G in Eq. (44) involves only ν as $\lambda/G=2\nu/(1-2\nu)$.

The displacement functions U_r, U_z, and U_θ are assumed as double summations of algebraic polynomials

$$U_r(\psi,\zeta) = \eta_r(\psi,\zeta)\sum_{i=0}^{I}\sum_{j=0}^{J} A_{ij}\,\psi^i\zeta^j,$$
$$U_z(\psi,\zeta) = \eta_z(\psi,\zeta)\sum_{k=0}^{K}\sum_{l=0}^{L} B_{kl}\,\psi^k\zeta^l,$$
$$U_\theta(\psi,\zeta) = \eta_\theta(\psi,\zeta)\sum_{m=0}^{M}\sum_{n=0}^{N} C_{mn}\,\psi^m\zeta^n, \tag{48}$$

where i, j, k, l, m, and n are integers; I, J, K, L, M, and N are the highest degrees taken in the polynomial terms; A_{ij}, B_{kl}, and C_{mn} are arbitrary coefficients to be determined; and the functions $\eta_{r,z,\theta}(\psi, \zeta)$ are depending upon the geometric boundary conditions to be enforced. For example,

1. completely free boundary conditions: $\eta_r=\eta_z=\eta_\theta=1$,
2. bottom edge fixed and remaining boundaries free: $\eta_r=\eta_z=\eta_\theta=\zeta-\zeta_b$,
3. top edge fixed and remaining boundaries free: $\eta_r=\eta_z=\eta_\theta=\zeta-\zeta_t$,

4. both top and bottom edges fixed: $\eta_r=\eta_z=\eta_\theta=(\zeta-\zeta_t)(\zeta-\zeta_b)$.

The eigenvalue problem is developed by minimizing the free vibration frequencies with respect to the arbitrary coefficients A_{ij}, B_{kl} and C_{mn}, thereby minimizing the effects of the internal constraints present, when the function sets are finite. This corresponds to the equations

$$\frac{\partial}{\partial A_{ij}}(V_{\max}-\omega^2 T^*_{\max})=0,\quad (i=0,1,2,\ldots,I;\ j=0,1,2,\ldots,J),$$

$$\frac{\partial}{\partial B_{kl}}(V_{\max}-\omega^2 T^*_{\max})=0,\quad (k=0,1,2,\ldots,K;\ l=0,1,2,\ldots,L),$$

$$\frac{\partial}{\partial C_{mn}}(V_{\max}-\omega^2 T^*_{\max})=0,\quad (m=0,1,2,\ldots,M;\ n=0,1,2,\ldots,N), \tag{49}$$

where $T_{\max}=\omega^2 T^*_{\max}$. The minimizing Eq. (49) yield a set of $(I+1)(J+1)+(K+1)(L+1)+(M+1)(N+1)$ linear, homogeneous, algebraic equations (or Ritz system) in the unknowns A_{ij}, B_{kl}, and C_{mn}. The equations can be written in the form $(\mathbf{K}-\Omega\mathbf{M})\mathbf{x}=0$, where $\mathbf{K}$ and $\mathbf{M}$ are stiffness and mass matrices resulting from the maximum strain energy ($V_{\max}$) and the maximum kinetic energy ($T_{\max}$), respectively, and Ω is the square of non-dimensional frequency $\omega^2 R_o^2\rho/G$, and the vector $\mathbf{x}$ is defined in the following form

$$\mathbf{x}=(A_{00},A_{01},\ldots,A_{IJ};B_{00},B_{01},\ldots,B_{KL};C_{00},C_{01},\ldots,C_{MN})^T. \tag{50}$$

In the present problem, the Ritz system has the following form

$$\begin{bmatrix} \mathrm{K}_{ij\hat{i}\hat{j}} & \mathrm{K}_{ijk\hat{l}} & \mathrm{K}_{ij\hat{m}\hat{n}} \\ \mathrm{K}_{kl\hat{i}\hat{j}} & \mathrm{K}_{kl\hat{k}\hat{l}} & \mathrm{K}_{kl\hat{m}\hat{n}} \\ \mathrm{K}_{mn\hat{i}\hat{j}} & \mathrm{K}_{mnk\hat{l}} & \mathrm{K}_{mn\hat{m}\hat{n}} \end{bmatrix}\begin{bmatrix} A_{\hat{i}\hat{j}} \\ B_{\hat{k}\hat{l}} \\ C_{\hat{m}\hat{n}} \end{bmatrix}=\Omega\begin{bmatrix} \mathrm{M}_{ij\hat{i}\hat{j}} & \mathbf{0} & \mathbf{0} \\ \mathbf{0} & \mathrm{M}_{kl\hat{k}\hat{l}} & \mathbf{0} \\ \mathbf{0} & \mathbf{0} & \mathrm{M}_{mn\hat{m}\hat{n}} \end{bmatrix}\begin{bmatrix} A_{\hat{i}\hat{j}} \\ B_{\hat{k}\hat{l}} \\ C_{\hat{m}\hat{n}} \end{bmatrix}, \tag{51}$$

where

$$\mathrm{K}_{ij\hat{i}\hat{j}}=\Gamma_1\left[\left(\frac{\lambda}{G}+2\right)\left(\frac{R_o}{H}\right)^2\left\langle P_{ij,\zeta},P_{\hat{i}\hat{j},\zeta}\right\rangle+\left\langle P_{ij,\psi},P_{\hat{i}\hat{j},\psi}\right\rangle\right]+n^2\Gamma_2\left\langle\frac{P_{ij}}{\psi},\frac{P_{\hat{i}\hat{j}}}{\psi}\right\rangle,$$

$$\mathrm{K}_{kl\hat{k}\hat{l}}=\Gamma_1\left[\left(\frac{\lambda}{G}+2\right)\left\{\left\langle\frac{P_{kl}}{\psi},\frac{P_{\hat{k}\hat{l}}}{\psi}\right\rangle+\left\langle P_{kl,\psi},P_{\hat{k}\hat{l},\psi}\right\rangle\right\}+\left(\frac{R_o}{H}\right)^2\left\langle P_{kl,\zeta},P_{\hat{k}\hat{l},\zeta}\right\rangle\right.$$
$$\left.+\left(\frac{\lambda}{G}\right)\left\{\left\langle\frac{P_{kl,\psi}}{\psi},P_{\hat{k}\hat{l}}\right\rangle+\left\langle\frac{P_{kl}}{\psi},P_{\hat{k}\hat{l},\psi}\right\rangle\right\}\right]+n^2\Gamma_2\left\langle\frac{P_{kl}}{\psi},\frac{P_{\hat{k}\hat{l}}}{\psi}\right\rangle,$$

$$\mathrm{K}_{mn\hat{m}\hat{n}}=n^2\Gamma_1\left(\frac{\lambda}{G}+2\right)\left\langle\frac{P_{mn}}{\psi},\frac{P_{\hat{m}\hat{n}}}{\psi}\right\rangle+\Gamma_2\left[\left(\frac{R_o}{H}\right)^2\left\langle P_{mn,\zeta},P_{\hat{m}\hat{n},\zeta}\right\rangle+\left\langle\frac{P_{mn}}{\psi},\frac{P_{\hat{m}\hat{n}}}{\psi}\right\rangle+\left\langle P_{mn,\psi},P_{\hat{m}\hat{n},\psi}\right\rangle\right.$$
$$\left.-\left\langle\frac{P_{mn}}{\psi},P_{\hat{m}\hat{n},\psi}\right\rangle-\left\langle\frac{P_{mn,\psi}}{\psi},P_{\hat{m}\hat{n}}\right\rangle\right],$$

$$\mathrm{K}_{ij\hat{k}\hat{l}}=\Gamma_1\left(\frac{R_o}{H}\right)\left[\left(\frac{\lambda}{G}\right)\left\{\left\langle\frac{P_{ij,\zeta}}{\psi},P_{\hat{k}\hat{l}}\right\rangle+\left\langle P_{ij,\zeta},P_{\hat{k}\hat{l},\psi}\right\rangle\right\}+\left\langle P_{ij,\psi},P_{\hat{k}\hat{l},\zeta}\right\rangle\right],$$

$$\mathrm{K}_{ij\hat{m}\hat{n}}=n\left(\frac{R_o}{H}\right)\left[\Gamma_1\left(\frac{\lambda}{G}\right)\left\langle\frac{P_{ij,\zeta}}{\psi},P_{\hat{m}\hat{n}}\right\rangle-\Gamma_2\left\langle\frac{P_{ij}}{\psi},P_{\hat{m}\hat{n},\zeta}\right\rangle\right],$$

$$\mathrm{K}_{kl\hat{m}\hat{n}}=n\Gamma_1\left[\left(\frac{\lambda}{G}+2\right)\left\langle\frac{P_{kl}}{\psi},\frac{P_{\hat{m}\hat{n}}}{\psi}\right\rangle+\frac{\lambda}{G}\left\langle\frac{P_{kl,\psi}}{\psi},P_{\hat{m}\hat{n}}\right\rangle\right]+n\Gamma_2\left[\left\langle\frac{P_{kl}}{\psi},\frac{P_{\hat{m}\hat{n}}}{\psi}\right\rangle-\left\langle\frac{P_{kl}}{\psi},P_{\hat{m}\hat{n},\zeta}\right\rangle\right],$$

$$\mathrm{M}_{ij\hat{i}\hat{j}}=\Gamma_1\left\langle P_{ij},P_{\hat{i}\hat{j}}\right\rangle,\qquad \mathrm{M}_{kl\hat{k}\hat{l}}=\Gamma_1\left\langle P_{kl},P_{\hat{k}\hat{l}}\right\rangle,\qquad \mathrm{M}_{mn\hat{m}\hat{n}}=\Gamma_2\left\langle P_{mn},P_{\hat{m}\hat{n}}\right\rangle, \tag{52}$$

where $P_{\alpha\beta}$ is defined by $P_{\alpha\beta}\equiv\psi^{\alpha}\zeta^{\beta}$ and $\mathrm{K}_{\alpha\beta\hat{\alpha}\hat{\beta}}$ and $\mathrm{M}_{\alpha\beta\hat{\alpha}\hat{\beta}}$ (α=i,k,m, β=j,l,n; $\hat{\alpha}=\hat{i},\hat{k},\hat{m}$, $\hat{\beta}=\hat{j},\hat{l},\hat{n}$) denote the submatrices of the stiffness and mass matrices, respectively. The symbol of < , > denotes an inner product defined by

$$\left\langle f,g\right\rangle\equiv\iint_{\Lambda}\eta(\psi,\zeta)\,f(\psi,\zeta)\,g(\psi,\zeta)\,\psi d\zeta d\psi\,. \tag{53}$$

For a nontrivial solution, the determinant of the coefficient matrix $|\mathbf{K}-\Omega\mathbf{M}|$ is set equal to zero, which yields the frequencies (eigenvalues). These frequencies are upper bounds of the exact values. The mode shape (eigenfunction) corresponding to each frequency is computed, in the usual manner, by substituting each Ω back into the set of algebraic equations, and solving for the ratios of coefficients.

3. Convergence study

To ensure the accuracy of frequencies computed by the procedure described above, it is necessary to carry out some convergence studies to decide the number of terms required in the power series of Eqs. (48). A convergence study is based on the fact that, if the displacements are expressed as power series, all the frequencies obtained by the Ritz method should converge to their exact values in an upper bound manner.

To make the study of convergence less complicated, equal numbers of polynomial terms were taken in both the r (or ψ) coordinate (i.e., I=K=M) and z (or ζ) coordinate (i.e., J=L=N), even though some computational optimization could be obtained for some configurations and some mode shapes by using unequal numbers of polynomial terms. The symbols ***TZ*** and ***TR*** in the tables stand for the total numbers of polynomial terms used through the axial (z or ζ) and the radial (r or ψ) directions, respectively. Note that the frequency determinant order ***DET*** is related to ***TZ*** and ***TR*** as follows

$$\boldsymbol{DET}=\begin{cases} TZ\times TR & \text{for torsional modes } (n=0^{\mathrm{T}}),\\ 2\times TZ\times TR & \text{for axisymmetric modes } (n=0^{\mathrm{A}}),\\ 3\times TZ\times TR & \text{for general modes } (n\geq 1). \end{cases} \tag{54}$$

Table 1 Convergence of frequencies $\omega R_o\sqrt{\rho/G}$ of a truncated (R_i/R_o=1/5) conical shell with variable thickness (h/H=1/5) free at the top edge and clamped at the bottom edge (F-C), for the five lowest bending modes for n=1 with α=30° and H/R_o=1/5 (ν=0.3)

TZ	***TR***	***DET***	**1**	**2**	**3**	**4**	**5**
4	**2**	**24**	1.530	2.490	3.241	4.205	4.549
4	**4**	**48**	1.513	2.384	3.076	3.903	4.202
4	**6**	**72**	1.511	2.367	3.022	3.786	4.178
4	**8**	**96**	1.510	2.366	3.016	3.752	4.172
4	**10**	**120**	1.510	2.366	3.015	3.750	4.169
4	**12**	**144**	1.510	2.366	3.015	3.750	4.169
5	**2**	**30**	1.529	2.476	3.200	4.139	4.262
5	**4**	**60**	1.512	2.366	3.026	3.814	4.186
5	**6**	**90**	**1.510**	2.365	3.016	3.746	4.171
5	**8**	**120**	1.510	2.364	3.013	3.743	4.168
5	**10**	**150**	1.510	2.364	3.013	3.742	4.168
5	**11**	**165**	1.510	2.364	3.013	3.742	**4.167**
5	**12**	**180**	1.510	2.364	3.013	3.742	4.167
6	**2**	**36**	1.528	2.469	3.172	4.073	4.246
6	**4**	**72**	1.511	2.365	3.016	3.749	4.173
6	**6**	**108**	1.510	2.364	3.014	3.743	4.169
6	**8**	**144**	1.510	**2.363**	3.013	3.742	4.168
6	**10**	**180**	1.510	2.363	3.013	**3.741**	4.167
6	**11**	**198**	1.510	2.363	**3.012**	3.741	4.167
6	**12**	**216**	1.510	2.363	3.012	3.741	4.167

TZ=Total numbers of algebraic polynomial terms used in the z (or ζ) direction
TR=Total numbers of algebraic polynomial terms used in the r (or ψ) direction
DET=Frequency determinant order

One sees in Table 1, for example, that the first non-dimensional frequency $\omega R_o\sqrt{\rho/G}$ for n=1 converges to four digits 1.510 when (TZ, TR)=(5,6) terms are used, which results in ***DET***=3×(5×6)=90.

Table 1 shows the convergence of non-dimensional frequencies $\omega R_o\sqrt{\rho/G}$ of a thick (H/R_o=1/5), truncated (R_i/R_o=1/5) conical shell of revolution with linear thickness variation (h/H=1/5) free at the top edge and clamped at the bottom edge (F-C) for the five lowest bending modes (n=1) with $\alpha = 30°$ for ν=0.3. It is seen in Table 1 that the frequencies have converged monotonically up to four significant figures as TZ (=J+1, L+1, and N+1 in Eqs. (48)) as well as TR (=I+1, K+1, and M+1 in Eqs. (48)) are increased. Underlined, bold-faced values in the table represent the converged results achieved with the smallest determinant size. The four-digit convergence for the first five frequencies requires determinants of order ***DET***=90 to 198.

4. Comparisons

Buchanan (2000) and Buchanan and Wong (2001) analyzed the truncated conical shells by a 3-D finite element method. The effects of different boundary conditions, including fixed-free and fixed-fixed, were studied. However, their works were all confined to the shells with *uniform*

Table 2 Comparisons of non-dimensional frequencies $\omega L\sqrt{\rho/G}$ of a truncated (R_i/L=0.25) conical shell with constant thickness (h/H=1) free at the top edge and clamped at the bottom edge (F-C) for H/L=0.25 and α=30° from the present 3-D Ritz method (3DR) and the 3-D finite element method (3DF) (v=0.3)

n	s	3DF	3DR	% Difference
0^{T}	1	2.435(3)	2.435	0%
	2	5.149	5.151	-0.04%
0^{A}	1	2.553(4)	2.555	-0.07%
	2	3.125	3.126	-0.03%
	3	3.980	3.981	-0.03%
	4	5.317	5.321	-0.08%
1	1	1.609(1)	1.608	0.06%
	2	2.866(5)	2.868	-0.07%
	3	3.430	3.429	0.03%
	4	4.456	4.457	-0.02%
	5	5.471	5.468	0.05%
	6	6.444	6.449	-0.08%
2	1	1.881(2)	1.880	0.05%
	2	3.161	3.164	-0.09%
	3	4.485	4.485	0%
	4	5.837	5.836	0.02%
	5	6.127	6.127	0%
	6	7.603	7.600	0.04%
3	1	3.149	3.149	0%
	2	4.463	4.465	-0.04%
	3	5.796	5.796	0%
	4	6.692	6.695	-0.04%
4	1	4.402	4.404	-0.05%
	2	6.196	6.201	-0.08%
	3	7.243	7.248	-0.07%
	4	7.903	7.910	-0.09%

n=circumferencial wave number; s=mode number

Table 3 Comparisons of non-dimensional frequencies $\lambda=\sqrt[4]{6\rho\omega^2(1-\nu)(R_o-H\cos\alpha/2)^4/GH^2}$ for torsional (n=0^T) and axisymmetric modes (n=0^A) of a truncated conical shell with linear thickness variation (h/H=1/2) clamped at the top edge and free at the bottom edge (C-F) with α=30°, H/R_o=0.09957, and R_i/R_o=0.4957 from the present 3-D Ritz method and 2-D shell theories (v=0.3)

n	s	3-D Present	2-D thin shell theories		
			Flügge theory	Love's first approximation theory	
			Irie *et al.*	Sankaranarayanan *et al.*	Viswanatham *et al.*
0^{T}	1	13.00	12.99	13.00	12.98
0^{A}	1	15.89	15.88	15.89	15.87
	2	17.57	17.57	17.57	17.57

n=circumferencial wave number; s=mode number

thickness. Table 2 shows comparisons of non-dimensional frequencies $\omega L\sqrt{\rho/G}$ of a truncated (R_i/L=0.25) conical shell of revolution with constant thickness (h/H=1) free at the top edge and

Table 4 Comparisons of non-dimensional frequencies $\omega R_o\sqrt{\rho/G}$ for the first five modes of annular plates ($\alpha\rightarrow 90°$) with linearly varying thickness for R_i/R_o=1/5, h/H=3, and H/R_o=1/9 (ν =0.3)

Boundary conditions	Methods	Mode sequence number				
		1	2	3	4	5
F-F	Present	0.6399	1.094	1.255	1.874	1.999
	(n,s)	(2,1)	(0^A,1)	(3,1)	(4,1)	(1,1)
	Taher *et al.*	0.6399	1.094	1.255	1.875	2.000
C-C	Present	2.378	2.426	2.790	3.534	3.757
	(n,s)	(0^A,1)	(1,1)	(2,1)	(3,1)	(0^T,1)
	Taher *et al.*	2.380	2.427	2.789	3.533	3.760
C-F	Present	0.7498	1.519	2.423	2.909	3.026
	(n,s)	(0^A,1)	(1,1)	(2,1)	(1,2)	(0^A,2)
	Taher *et al.*	0.7499	1.518	2.423	2.908	3.024

F-F: Completely free
C-C: Clamped inner edge and clamped outer edge
C-F: Clamped inner edge and free outer edge
n=circumferencial wave number; s=mode number

clamped at the bottom edge (F-C) for H/L=0.25 and α=30° from the present 3-D Ritz method and the 3-D finite element method (Buchanan and Wong 2001) for ν=0.3, where L is equal to csc $\alpha(R_o-R_iH\cos\alpha)$ as the slant length of the truncated conical shell. The percent difference in frequencies obtained by the present 3-D Ritz analysis (3DR) and the 3-D finite element method (3DF) is given by

$$\text{Difference (\%)}=\frac{\text{3DF}-\text{3DR}}{\text{3DR}}\times 100\ . \tag{55}$$

The table shows good agreement in frequencies. The 1st and 2nd frequencies from 3DR are smaller than those from 3DF.

Some researchers (Irie *et al.* 1982, Sankaranarayanan *et al.* 1987, Viswanatham and Navaneethakrishnan 2005) investigated the natural frequencies of truncated conical shells with linear thickness variation based upon 2-D thin shell theories of Flügge theory (Irie *et al.* 1982) or Love's first approximation theory (Sankaranarayanan *et al*. 1987, Viswanatham and Navaneethakrishnan 2005). Table 3 shows comparisons of non-dimensional frequencies

$$\lambda=\sqrt[4]{6\rho\omega^2(1-\nu)(R_o-H\cos\alpha/2)^4/GH^2} \tag{56}$$

for torsional (n=0^T) and axisymmetric modes (n=0^A) of truncated conical shell with linear thickness variation (h/H=1/2) clamped at the top edge and free at the bottom edge (C-F) with α=30°, H/R_o=0.09957, and R_i/R_o=0.4957 from the present 3-D Ritz method and 2-D shell theories (Irie *et al.* 1982, Sankaranarayanan *et al*. 1987, Viswanatham and Navaneethakrishnan 2005) for ν=0.3. The table shows good agreement in frequencies. However, it is strange that some of the frequencies by the present 3-D analyses are larger than those by 2-D shell theories, mainly because shear deformation and rotary inertia effects are accounted for in a 3-D analysis, but not in most of 2-D thin shell theories.

Taher *et al*. (2006) computed the natural frequencies of circular and annular plates with variable

thickness and combined boundary conditions using 3-D elasticity theory. An annular plate with variable thickness is a special case of a truncated conical shells with variable thickness when $\alpha \to 90°$. Table 4 shows comparisons of non-dimensional frequencies $\omega R_o\sqrt{\rho/G}$ for the first five modes of annular plates with linearly varying thickness for R_i/R_o=1/5, h/H=3, H/R_o=1/9, and v=0.3 from the present 3-D method and their 3-D study. The table shows very good agreement in frequencies irrespective of the boundary conditions.

Table 5 Non-dimensional frequencies $\omega R_o\sqrt{\rho/G}$ of truncated (R_i/R_o=1/5) conical shells with linear thickness variation (h/H=1/5) free at the top edge and clamped at the bottom edge (F-C) with H/R_o=1/5 (v=0.3)

n	***s***	α				
		15°	30°	45°	60°	75°
0^{T}	**1**	1.313(5)	2.502(7)	3.465(9)	4.133(9)	4.477(10)
	2	2.305	4.388	6.066	7.222	7.806
	3	3.354	6.377	8.801	10.46	11.27
	4	4.453	8.461	11.66	13.84	14.90
	5	5.583	10.60	14.61	17.32	18.62
0^{A}	**1**	1.519(7)	2.464(6)	2.366(4)	2.001(3)	1.381(1)
	2	2.344	2.710(8)	3.170(7)	3.033(5)	2.714(4)
	3	2.636	3.549	4.305	4.744	4.957
	4	3.121	4.378	5.228	5.743	6.082
	5	3.481	5.262	6.047	7.195	7.817
1	**1**	0.6577(1)	1.510(2)	1.898(2)	1.839(1)	1.491(2)
	2	1.208(4)	2.363(5)	3.062(6)	3.126(6)	2.937(6)
	3	1.902(10)	3.012	3.655	4.166(10)	4.454(9)
	4	2.493	3.741	4.453	4.909	5.151
	5	2.616	4.167	5.025	5.697	6.053
2	**1**	0.7419(2)	1.197(1)	1.635(1)	1.882(2)	1.939(3)
	2	1.071(3)	1.983(4)	2.805(5)	3.326(7)	3.528(7)
	3	1.521(8)	3.102	4.325	4.976	5.115
	4	2.108	4.334	5.092	5.452	5.725
	5	2.755	4.646	6.247	6.866	7.083
3	**1**	1.431(6)	1.906(3)	2.318(3)	2.615(4)	2.753(5)
	2	1.898(9)	2.756(9)	3.544(10)	4.166(10)	4.505
	3	2.365	3.693	5.056	6.038	6.497
	4	2.806	4.879	6.436	6.687	6.732
	5	3.276	5.887	6.969	8.355	8.588
4	**1**	2.307	2.846(10)	3.289(8)	3.592(8)	3.722(8)
	2	2.902	3.926	4.774	5.397	5.728
	3	3.477	4.984	6.275	7.278	7.820
	4	4.044	6.038	7.775	8.098	8.150
	5	4.605	7.142	8.012	9.499	10.21

T=Torsional mode; A=Axisymmetric mode.
Numbers in parentheses identify frequency sequence.

Table 6 Non-dimensional frequencies $\omega R_o\sqrt{\rho/G}$ of truncated (R_i/R_o=1/5) conical shells with linear thickness variation (h/H=1/10) free at the top edge and clamped at the bottom edge (F-C) with H/R_o=1/5 (v=0.3)

n	s	α				
		15°	30°	45°	60°	75°
$\mathbf{0^T}$	**1**	1.274(10)	2.445	3.425	4.144	4.558
	2	2.216	4.254	5.955	7.201	7.914
	3	3.181	6.104	8.542	10.32	11.34
	4	4.178	8.016	11.21	13.54	14.87
	5	5.201	9.977	13.95	16.85	18.49
$\mathbf{0^A}$	**1**	1.479	2.171	2.022(7)	1.654(4)	1.086(3)
	2	2.097	2.454	2.595	2.361(9)	1.741(5)
	3	2.301	2.915	3.370	3.222	2.745
	4	2.627	3.417	4.105	4.199	4.308
	5	2.900	4.047	4.891	5.688	6.132
1	**1**	0.6381(2)	1.402(4)	1.633(3)	1.463(3)	1.039(1)
	2	1.128(8)	2.077(10)	2.413(10)	2.289(8)	1.768(6)
	3	1.694	2.530	3.145	3.162	2.810
	4	2.100	3.078	3.697	4.235	4.384
	5	2.423	3.495	4.139	4.240	4.601
2	**1**	0.3920(1)	0.8267(1)	1.145(1)	1.198(1)	1.052(2)
	2	0.6709(3)	1.424(6)	1.907(6)	2.038(6)	1.860(8)
	3	1.073(6)	2.149	2.794	3.041	3.006
	4	1.516	2.866	3.787	4.317	4.612
	5	1.940	3.617	4.774	5.101	5.231
3	**1**	0.6994(4)	0.9497(2)	1.186(2)	1.333(2)	1.374(4)
	2	0.9029(5)	1.361(3)	1.833(5)	2.117(7)	2.199(10)
	3	1.080(7)	1.969(8)	2.741	3.199	3.377
	4	1.361	2.703	3.815	4.575	4.994
	5	1.722	3.508	5.051	6.251	6.580
4	**1**	1.135(9)	1.417(5)	1.654(4)	1.826(5)	1.913(9)
	2	1.414	1.869(7)	2.283(9)	2.619	2.803
	3	1.660	2.301	3.062	3.639	3.942
	4	1.839	2.927	4.120	5.024	5.534
	5	2.042	3.710	5.395	6.729	7.526
5	**1**	1.678	2.005(9)	2.274(8)	2.467(10)	2.567
	2	2.028	2.598	3.047	3.394	3.601
	3	2.345	3.068	3.744	4.343	4.698
	4	2.630	3.549	4.708	5.670	6.233
	5	2.853	4.246	5.956	7.354	8.186

T=Torsional mode; A=Axisymmetric mode.
Numbers in parentheses identify frequency sequence.

5. Numerical results

Tables 5 and 6 present the non-dimensional frequencies $\omega R_o\sqrt{\rho/G}$ of truncated (R_i/R_o=1/5) conical shells with linear thickness variation along the meridional direction free at the top edge and

clamped at the bottom edge (F-C) for α=15°, 30°, 45°, 60°, 75° with $h/H=H/R_o$=1/5 in Table 5 and $h/H=H/R_o$=1/10 in Table 6 for ν=0.3. The conical shell configurations for Table 5 are depicted in Fig. 2. The mode shapes of the conical shells at $z=z_0$ are given in Fig. 3 for each value of n except for the torsional ones ($n=0^T$). The mode shapes have 2n nodal points (u_r=0) for each n. Thirty frequencies are given for each shell configuration, which arise from six circumferential wave numbers ($n=0^T$, 0^A, 1, 2, 3, 4) and the first five modes (s=1, 2, 3, 4, 5) for each value of n, where the superscripts T and A indicate torsional and axisymmetric modes, respectively. The numbers in parentheses identify the first ten frequencies for each shell configuration. For example, in the case of α=15° in the first column of Table 5, the first ten frequencies are modes for (n,s) = (1,1), (2,1), (2,2), (1,2), (0^T,1), (3,1), (0^A,1), (2,3), (3,2), (1,3) in this order.

It is seen in Tables 5 and 6 that most of the frequencies become larger as α increases. It is also observed that the torsional ($n=0^T$) modes are more important as α becomes smaller, and the axisymmetric ($n=0^A$) modes are more important as α becomes larger. The modes for higher circumferential wave number of relatively thin conical shells (H/R_o=1/10) are more important

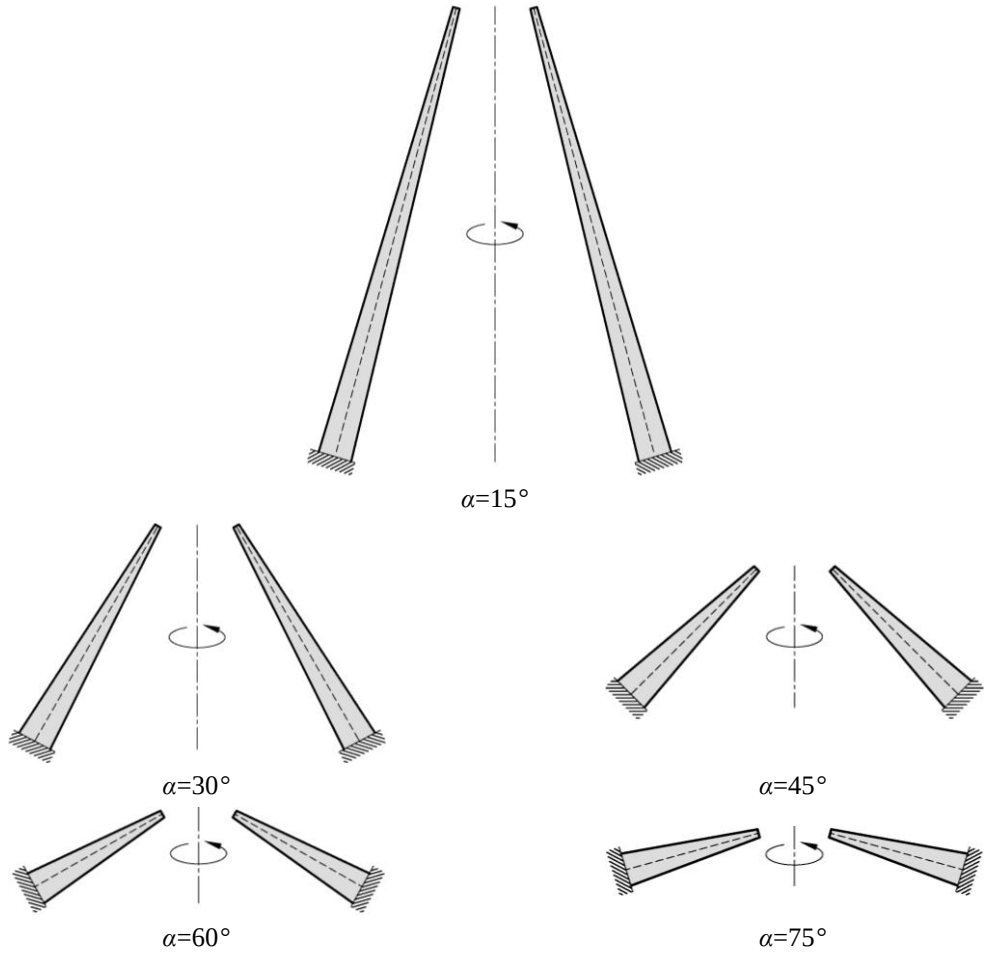

Fig. 2 Cross-sections of truncated, free-clamped (F-C) conical sells having linear thickness variation for R_i/R_o=1/5, h/H=1/5, and H/R_o=1/5

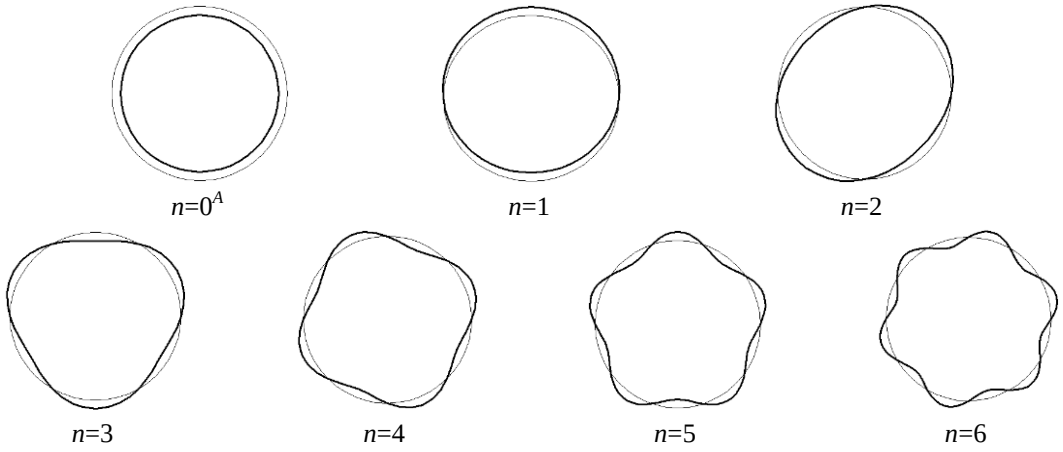

Fig. 3 Mode shapes for each n

compared with those of thick conical shells (H/R_o=1/5). That is, they are among the lowest frequencies of the conical shells.

6. Conclusions

Accurate frequency data determined by the 3-D Ritz analysis have been presented for truncated shallow and deep conical shells with linear thickness variation along the meridional direction free at the top edge and clamped at the bottom edge. The present analysis is based on the circular cylindrical coordinate system instead of the conical one, mainly because the latter takes more time to compute the energy integration numerically than based on the former. The analysis uses the 3-D equations of the theory of elasticity in their general forms for isotropic materials. They are only limited to small strains. No other constraints are placed on the displacements. This is an obvious difference between the 3-D analysis and the classical 2-D thin shell theories, which make very limiting assumptions about the displacement variation through the shell thickness.

The method is able to determine frequencies as close to the exact ones as wanted. Therefore, the data in Tables 5 and 6 may be regarded as benchmark results against which 3-D results obtained by other methods, such as finite elements and finite differences, may be compared to determine the accuracy of the latter. Moreover, the frequency determinants required by the present method are at least an order of magnitude smaller than those needed by finite element analyses of comparable accuracy. McGee and Leissa (1991) demonstrated extensively in their paper. The Ritz method guarantees upper bound convergence of the frequencies in terms of functions sets that are mathematically complete, such as algebraic polynomials. Some finite element methods can also accomplish this, but at much greater costs, and others cannot.

Acknowledgments

This research was supported by the Chung-Ang University research grant in 2016.

References

Buchanan, G.R. (2000), "Vibration of truncated conical cylinders of crystal class 6/mmm", *J. Vib. Control*, **6**, 985-998.

Buchanan, G.R. and Wong, F.T.I. (2001), "Frequencies and mode shapes for thick truncated hollow cones", *Int. J. Mech. Sci*., **43**, 2815-2832.

Irie, T., Yamada, G. and Kaneko, Y. (1982), "Free vibration of a conical shell with variable thickness", *J. Sound Vib*., **82**(1), 83-94.

Jin, G., Ma, X., Shi, S., Ye, T. and Liu, Z. (2014a), "A modified Fourier series solution for vibration analysis of truncated conical shells with general boundary conditions", *Appl. Acoust*., **85**, 82-96.

Jin, G., Su, Z., Shi, S., Ye, T. and Gao, S. (2014b), "Three-dimensional exact solution for the free vibration of arbitrarily thick functionally graded rectangular plates with general boundary conditions", *Compos. Struct*., **108**, 565-577.

Jin, G., Xie, X. and Liu, Z. (2014c), "The Haar wavelet method for free vibration analysis of functionally graded cylindrical shells based on the shear deformation theory", *Compos. Struct*., **108**, 435-448.

Jin, G., Ye, T., Chen, Y., Su, Z. ad Yan, Y. (2013a), "An exact solution for the free vibration analysis of laminated composite cylindrical shells with general elastic boundary conditions", *Compos. Struct*., **106**, 114-127.

Jin, G, Ye, T., Jia, X. and Gao, S. (2014), "A general Fourier solution for the vibration analysis of composite laminated structure elements of revolution with general elastic restraints", *Compos. Struct.*, **109**, 150-168.

Jin, G., Ye, T., Ma, X., Chen, Y., Su, Z. and Xie, X. (2013b), "A unified approach for the vibration analysis of moderately thick composite laminated cylindrical shells with arbitrary boundary conditions", *Int. J. Mech. Sci*., **75**, 357-376.

Leissa, A.W. (1993), *Vibration of shells*, The Acoustical Society of America.

Leissa, A.W. and So, J. (1995), "Three-dimensional vibrations of truncated hollow cones", *J. Vib. Control*, **1**, 145-158.

Malekzadeh, P., Fiouz, A.R. and Sobhrouyan, M. (2012), "Three-dimensional free vibration of functionally graded truncated conical shells subjected to thermal environment", *Int. J. Pres. Vess. Pip*., **89**, 210-221.

McGee, O.G. and Leissa, A.W. (1991), "Three-dimensional free vibrations of thick skewed cantilever plates", *J. Sound Vib*., **144**, 305-322.

Sankaranarayanan, N., Chandrasekaran, K. and Ramaiyan, G. (1987), "Axisymmetric vibrations of laminated conical shells of variable thickness", *J. Sound Vib*., **118**(1), 151-161.

Sofiyev, A.H. (2014a), "Large-amplitude vibration of non-homogeneous orthotropic composite truncated conical shell", *Compos. Part B: Eng*., **61**, 365-374.

Sofiyev, A.H. (2014b), "The influence of non-homogeneity on the frequency–amplitude characteristics of laminated orthotropic truncated conical shell", *Compos. Struct*., **107**, 334-345.

Su, Z., Jin, G., Shi, S., Ye, T. and Jia, X. (2014a), "A unified solution for vibration analysis of functionally graded cylindrical, conical shells and annular plates with general boundary conditions", *Int. J. Mech. Sci*., **80**, 62-80.

Su, Z., Jin, G. and Ye, T. (2014b), "Three-dimensional vibration analysis of thick functionally graded conical, cylindrical shell and annular plate structures with arbitrary elastic restraints", *Compos. Struct*., **118**, 432-447.

Qu, Y., Long, X., Yuan, G. and Meng, G. (2013a), "A unified formulation for vibration analysis of functionally graded shells of revolution with arbitrary boundary conditions", *Compos. Part B: Eng*., **50**, 381-402.

Qu, Y., Long, X., Wu, S. and Meng, G. (2013b), "A unified formulation for vibration analysis of composite laminated shells of revolution including shear deformation and rotary inertia", *Compos. Struct*., **98**, 169-191.

Taher, H.R.D., Omidi, M., Zadpoor, A.A. and Nikooyan, A.A. (2006), "Free vibration of circular and annular plates with variable thickness and different combinations of boundary conditions", *J. Sound Vib*., **296**,

1084-1092.
Viswanatham, K.K. and Navaneethakrishnan, P.V. (2005), "Free vibration of layered truncated conical shell frusta of differently varying thickness by the method of collocation with cubic and quintic splines", *Int. J. Solid. Struct*., **42**, 1129-1150.
Ye, T., Jin, G., Chen, Y., Ma, X. and Su, Z. (2013), "Free vibration analysis of laminated composite shallow shells with general elastic boundaries", *Compos. Struct*., **106**, 470-490.
Ye, T., Jin, G., Shi, S. and Ma, X. (2014), "Three-dimensional free vibration analysis of thick cylindrical shells with general end conditions and resting on elastic foundations", *Int. J. Mech. Sci*., **84**, 120-137.

CC